J Electr Eng Technol.2018; 13(1): 001-010
http://doi.org/10.5370/JEET.2018.13.1.001

ISSN(Print) 1975-0102
ISSN(Online) 2093-7423

A Framework for Wide-area Monitoring of Tree-related High Impedance Faults in Medium-voltage Networks

N. Bahador*, H.R. Matinfar† and F. Namdari*

Abstract – Wide-area monitoring of tree-related high impedance fault (THIF) efficiently contributes to increase reliability of large-scaled network, since the failure to early location of them may results in critical lines tripping and consequently large blackouts. In the first place, this wide-area monitoring of THIF requires managing the placement of sensors across large power grid network according to THIF detection objective. For this purpose, current paper presents a framework in which sensors are distributed according to a predetermined risk map. The proposed risk map determines the possibility of THIF occurrence on every branch in a power network, based on electrical conductivity of trees and their positions to power lines which extracted from spectral data. The obtained possibility value can be considered as a weight coefficient assigned to each branch in sensor placement problem. The next step after sensors deployment is to on-line monitor based on moving data window. In this on-line process, the received data window is evaluated for obtaining a correlation between low frequency and high frequency components of signal. If obtained correlation follows a specified pattern, received signal is considered as a THIF. Thereafter, if several faulted section candidates are found by deployed sensors, the most likely location is chosen from the list of candidates based on predetermined THIF risk map.

Keywords: Wide-area monitoring, Tree-related high impedance fault, Off-line mapping, Spectral data

1. Introduction

THE issue of high impedance faults has been one of the most challenging problems in power distribution systems. These kinds of faults which comprise about 10 percent of the distribution faults have current magnitude close to the load current level or even lower and therefor are not detectable by over-current protection devices [1-3]. This research is just focused on the HIF current that passes through live vegetation. It occurs when power line transiently come in contact with live trees. The reason for making this choice is that tree-power line contact is the major cause of power outages in the United States according to the Edison Electric Institute (Fig. 1).

The earlier studies in the field of high impedance fault have considered various methods for HIFs detection. But the problem of these HIF detection methods was in using same detection/location techniques for all types of HIF. These detection methods have been proposed based on conventional HIF models which can't represent the expected behavior of a THIFs. Following reasons justify why these methods are not applicable for THIF detection:

1. Previous HIF detection methods are based on conventional models of HIF. Most of these models represent the behavior of arc [5-9]. While arc does not occur during initial cycles of THIF. An arc will occur when the moisture of tree's bark is expulsed and ignition process is started. Electric arcs occur in the flame along the tree's branch and this causes large fluctuations in the current waveform. As shown in Fig. 2, it takes about 20-30 seconds for arcs to happen.
2. One other feature of THIF that differentiates it from other HIFs, is the moisture expulsion from the outermost layer of bark in the form of steam which accompanied by a continuous audible whistling noise. During the expulsion of moisture, a considerable reduction from first peak is seen in the current RMS [4]. As shown in Fig. 1, it occurs before the arcs occurrence commenced. This reduction is not seen in current RMS of other HIFs.

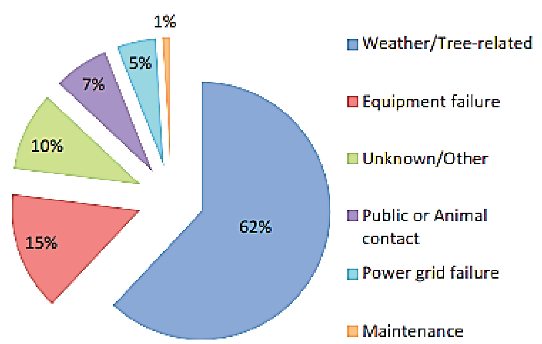

Fig. 1. Power outages causes in the United States [4]

† Corresponding Author: Dept. of Remote Sensing, GIS and Soil Science, Lorestan Univerity, Iran. (matinfar44@gmail.commailto, gilsoon@kiee.or.kr)
* Dept. of Electrical Engineering, Lorestan University, Iran. (nu.bahador@yahoo.com, Namdari.f@lu.ac.ir)
Received: February 18, 2017; Accepted: July 18, 2017

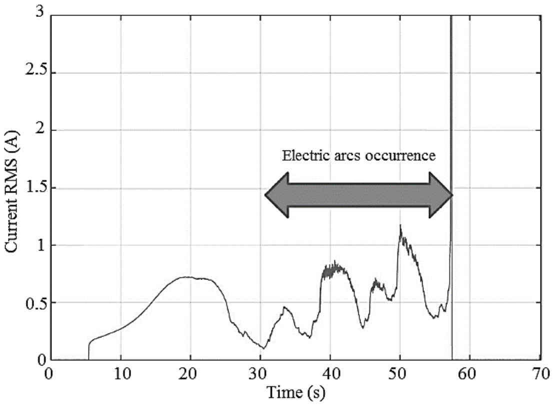

(a) The case study of Manna Gum tree [4]

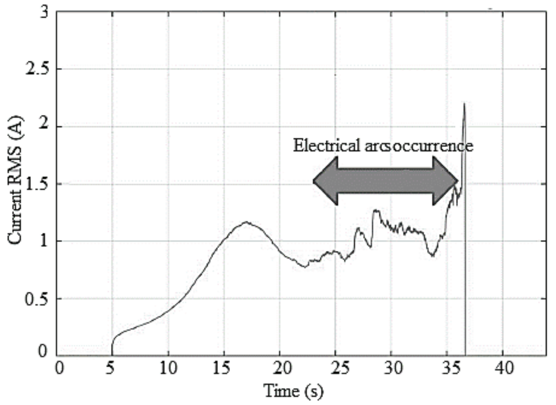

(b) The case study of Golden Wattle tree [4]

Fig. 2. Current RMS of a THIF

3. The high-frequency components of THIF current is generally much smaller than other types of HIF [4].
4. At the first cycles of THIF, tree acts as a linear resistor with low distortion. While conventional models represent nonlinear behavior of HIFs [10, 11].
5. The rate of growth of current is much faster in other types of HIFs than in THIF [12]. Although a flashover occurs too rapidly in the case of other HIFs like fallen conductor, it takes several tens of seconds for THIF current to develop to flashover.

Considering the differences between various types of high impedance faults, it is important to separately address each type of HIF. In other words, there should be distinct criteria for detecting each type of HIF.

In addition to the above differences, the other problem with previous detection methods is that about 40 percent of all feature extraction methods for the high impedance faults have been wavelet-based techniques [13-16]. When a signal transfers to a new domain such as wavelet domain, some characteristics of the original signal will be lost and cannot be effectively evaluated. This is due to the fact that the decomposed functions of a signal in wavelet domain are not of the same length as the original signal. For this reason, varying frequency in time may not be preserved. That is why the data may be lost in the wavelet domain. These techniques (Wavelet-based technique) have low ability for feature extraction, and are so dependent on types of mother wavelet. While a technique like empirical mode decomposition (EMD) does not have such problems and keeps signals in their own domain [17, 18]. Therefore, EMD is used as an applicable tool for feature extraction of tree-related high impedance faults in this paper. The basis of the empirical mode decomposition is evaluation of local oscillations in the signal. This method studies the trend of variations in the signal between two sequential local extrema so that the details and features of original signal are extracted.

Therefore, for all the reasons mentioned above, the aim of this paper is first to study a new method for detecting THIF.

Beside feature extraction problem, the more serious issue is low efficiency of available HIF location methods in facing with environmental noise [19]. Given the importance of mentioned issue, the main purpose of current paper is to improve the efficiency of detecting and locating tree-related HIF especially in large-scale MV networks. To achieve this goal, a series of experiments and preliminary studies are done in this paper in order to reach to an accurate tree-related HIF mapping. In situations where there is the possibility of sending wrong tree-related HIF signal, the offline mapping system of tree-related HIF helps to increase the accuracy of detection / location techniques. The findings of this study can be effective in Wide-area monitoring of high impedance faults. The most obvious advantage of suggested scheme is proposing the use of satellite imagery in mapping which is economically advantageous in large-scale. This mapping provides a cost-effective, useful tool for THIF sensors placement and improving decision making processes to organize early THIF warning. Using these maps is helpful in assessing the spatiotemporal distribution of THIF risk using spectral data.

The possibility of electrical arcs occurrence near vegetation and electrical current passing through them found to increase as electrical conductivity of vegetation increases. At very low electrical conductivity levels, vegetation acts as an electrical insulator and does not conduct enough electrical current to THIF occurrence. When vegetation gets too close to medium voltage or high voltage power lines, it is possible that a transient electrical leakage current occurs and vegetation provides a path for low electrical current to flow. Heating during electrical current leakage causes carbonization of vegetation's tissues. The carbonized path results in increase in electrical conductivity of vegetation and consequently provides lower resistance to the electrical leakage current. As time go on, it becomes more possible that a flashover occurs [20].

Different tree species coming in contact with power lines show widely varying THIF risk [20]. So determination of species around power lines which are the most likely to conduct electricity is important for the spatiotemporal distribution of THIF risk. The common techniques to estimate electrical conductivity of vegetation are to make field surveys and collect samples that are so costly and time consuming, and it is difficult to extrapolate them over space and time. This is why the fitting models to estimate vegetation's electrical conductivity using spectral data that could be more easily and quickly measured, is considered a useful tool for hazard management. This type of estimation could be temporally extended and spatially generalized.

The electrical conductivity of vegetation can be determined using remote sensing methods as its variations affect the vegetation's spectral signature. To this end, in this study, a mathematical model is fitted using spectral indices and field estimations of electrical conductivity values. This study is the first attempt to monitor electrical conductivity of live trees in the power lines' corridors using satellite imagery.

2. Off-line Mapping of Tree-related HIF in MV Networks

Since power grid become more widespread, conventional surveys of power line corridor using ground/aerial patrol inspection are so costly and time consuming. This is why the utilization of satellite images due to wide area coverage, frequent overhead passes, the ability to view areas with restricted physical access, and potential lower cost from processing a large area at one time in an automated workflow, is considered a useful tool for risk mapping in current paper. This proposed risk mapping determines the coordinates of THIF danger zones based on electrical conductivity of trees and their proximity to the power lines. The novelty of this section is recommending electrical conductivity of hazardous trees (trees within a close enough proximity to the power line) as an indicator of THIF risk. To this end, visible and near infrared spectral bands of Sentinel-II are analyzed in order to study the relationship of spectral data and electrical conductivity component of trees' crown.

2.1 Trees' location map

The study area is in one part of the Heydareh rural road located in Hamedan, Iran (Fig. 3).

To report hazardous positions of trees, all objects of image except trees should be excluded in order to obtain accurate map of trees' location. Then after, trees in a close enough proximity to the power lines are determined by integrating obtained map and power grid map.

Wavelet transform is used to remove unnecessary objects from image. This paper apply Daubechies-10 wavelet transform which is found superior to all other approaches in decomposing image. As low decomposition levels result in poor spatial quality, eighth level wavelet decomposition is applied to image to achieve high accuracy. In order to reduce the computational load, panchromatic image of study area with the color number of 15 is decomposed. The reconstructed version of the second level component of decomposed image show trees' crowns that are completely distinct from other features in original image (Fig. 4).

2.2 Trees' electrical conductivity map

The sap content passing through vascular structure plays the role of electrical conductor [20], and its electrical conductivity should therefore be measured. According to this point, the leaf xylem content alone was sufficient to consider for measuring tree's electrical conductivity.

The field estimation was conducted in December 2016 in which the sampling was consisted of random collecting the fresh leaves of studied poplar trees. The distribution of these sampling points is plotted in Fig. 5. Samples were collected between 11 A.M. and 2 P.M. and transported in sealed bags to the laboratory. For measuring the electrical conductivity of samples, 0.1 g of each sample was cut and

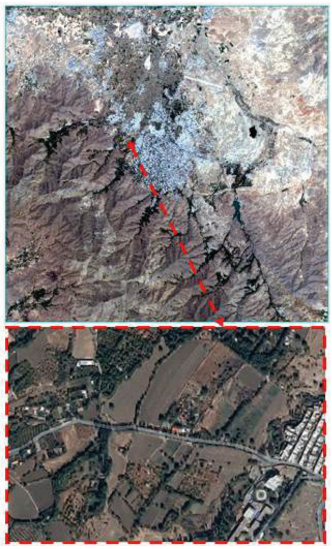

Fig. 3. Study area

Fig. 4. Obtained white points representing trees' crown in Fig. 3

Fig. 5. Location of sampling points

(a) Weighting one piece of leaf (0.1 g) and crushing it

(b) Providing 10 ml of double distilled water and adding it to crushed leaf

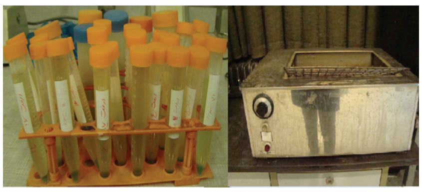

(c) Taking obtained solutions into tubes and keeping them at 40 °C for 30 minute in Bain Marie

Fig. 6. Electrical conductivity measurement of samples

taken into tubes with 10 ml of double distilled water [22]. The tubes were kept at 40 °C for 30 minute in Bain Marie and then their electrical conductivity was measured by EC meter. The procedures of performed experimental tests are documented in Fig. 6.

In order to measuring EC, 25 trees were selected and 20 leave samples were taken from each tree. Thereafter, the electrical conductivity values of 20 samples related to each tree were measured in laboratory, and their average value

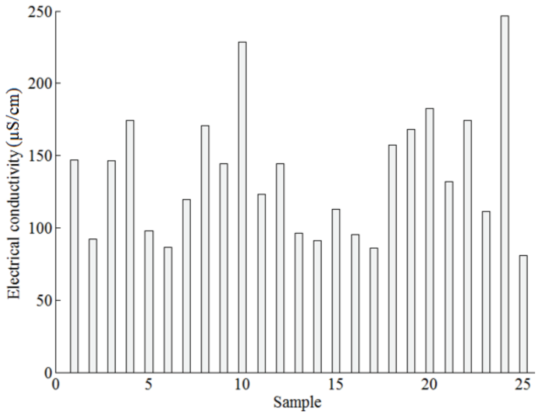

Fig. 7. EC values of 25 live poplar trees

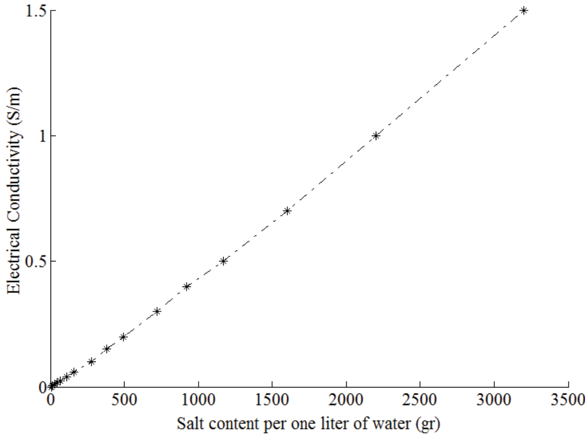

Fig. 8. Linear relationship between electrical conductivity and salt content of an electrolyte

was calculated. Fig. 7 summarizes the results from field investigation and laboratory measurements of 25 live poplar trees.

As mentioned previously, what could be effective on electrical conductivity of vegetation is the electrolyte content transported in Xylems [20, 21]. As shown in Fig. 8, there is a linear relationship between electrical conductivity and salt content of an electrolyte solution. Furthermore, experiments have also demonstrated the observance of Ohm's law for electrolyte solutions even at the lowest intensities [23]. Therefore, according to the above point and inasmuch as the electrical conductivity of leaf water content approximately represents the level of electrolytic in tree's vascular water and consequently represents the electrical conductivity of the whole tree, there would be a linear relationship between electrical conductivity of leaf water content with the HIF current amplitude.

To estimate electrical conductivity of trees from satellite image, the spectral indices were calculated using data set of cloud-free Sentinel-II image at a spatial resolution of 10 m that was composed of four spectral bands of 490 nm (band 1-blue), 560 nm (band 2-green), 665 nm (band 3-red) and 842 nm (band 4-infrared). This image was acquired in

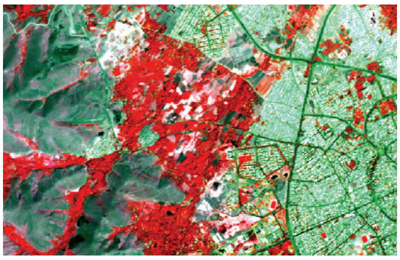

Fig. 9. False color composite (432) of study area

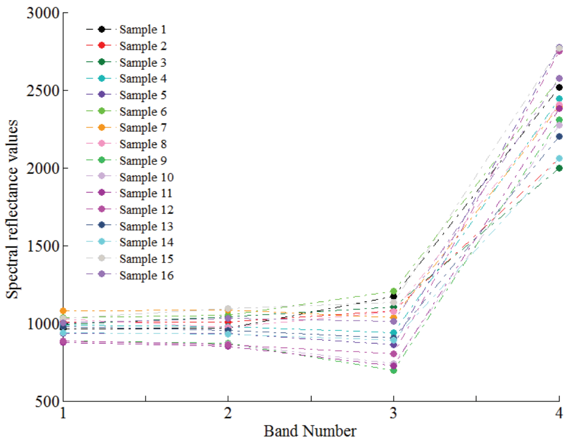

Fig. 10. The reflectance data corresponding to each spectral band

December 2016. Fig. 9 shows the false color composite 432 (Infrared-Red-Green) of study area.

The exact coordinates of each sampling point were recorded using the global positioning system (GPS) and their corresponding reflectance data were extracted from false color composite image for each spectral band (Fig. 10).

Different combinations of reflectance data corresponding to each wavelength were analyzed to look for a relationship between the electrical conductivity values of samples and corresponding values of extracted spectral index, and the best of them with highest coefficient of determination (R^2) was selected. The proposed spectral index which extracted from the full spectral bands is defined as:

$$x = \{(R_4 - R_3) \times (R_2 - R_1)\} \quad (1)$$

where R_1 to R_4 are the reflectance corresponding to the wavelengths of 490, 560, 665 and 842 nm, respectively.

Regression analysis was then used to evaluate the correlation between electrical conductivity values and extracted spectral variable. The strength of correlation between measured and predicted variables was indicated using the R^2 value.

The obtained equation to estimate electrical conductivity (μS/cm) of live trees using spectral indices is as follows. x_n is spectral reflectance value related to band n^{th}. The coefficients of this regression equation are given in Table 1.

Table. 1. Coefficients of regression equation

Coefficient	Value	Coefficient	Value
a_1	3210	b_3	0.000163
a_2	3097	c_1	1.486
a_3	15.21	c_2	-1.665
b_1	9.996e-06	c_3	-0.3016
b_2	1.032e-05		

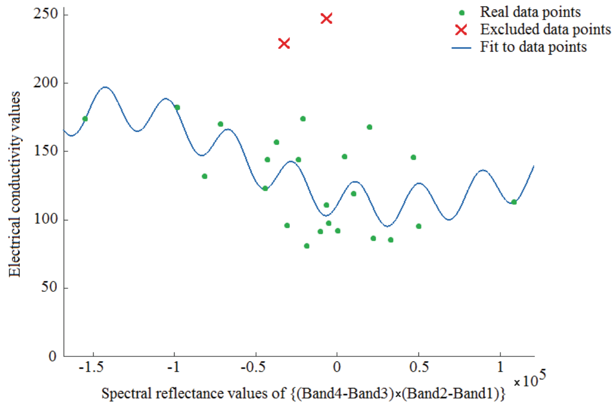

Fig. 11. The model fitted for electrical conductivity with the $R^2 = 0.4409$

$$EC = a_1 Sin(b_1 x + c_1) + a_2 Sin(b_2 x + c_2) + a_3 Sin(b_3 x + c_3) \quad (2)$$

$$x = (x_4 - x_3) \times (x_2 - x_1) \quad (3)$$

The model fitted for electrical conductivity is presented in Fig. 11 with the R^2=0.4409. According to this coefficient of determination, a desired level of accuracy was achieved by this fitting.

According to above findings, the coordinates of THIF danger zones based on electrical conductivity of trees and their proximity to the power lines could be easily determined. The higher the electrical conductivity and the lower the distance to power lines, the more hazardous a vegetation is.

3. Maximum Amplitude Determination of High Frequency Components due to Tree-related HIF

Thereafter the hazardous tree is identified, the maximum amplitude of high frequency component and fundamental part of THIFs that could be generated by this tree is estimated as follow. Being aware of the contribution of each hazardous tree to cause THIF before it happens, could be so helpful for monitoring target.

Table 2. Max amplitude of THIF current (A)

Tree species	Electrical conductivity (μs/cm)	Maximum THIF current	
		FEM results	Experimental results
Walnut	231.7	0.5299	0.5098
Poplar	218.1	0.4988	0.4521

Table 3. Max amplitude of THIF current

Species	The level of fundamental component (A)	The level of high frequency components (A)	Ratio of high frequency components' pulses to fundamental component (%)
Walnut	0.4706	0.0424	9.00
Poplar	0.4422	0.0245	5.54
Ash	0.3182	0.0329	10.33

3.1 Maximum amplitude determination of fault current

The electrical conductivity of tree is applied to finite element analysis as input data and the maximum amplitude of tree-related HIF is calculated.

For finite element analysis, tree trunk structure is assumed as a truncated cones and boundary conditions are specified as voltage and current density of conductors and the ground voltage [20].

For assessing the validity of the FEM results in estimating maximum amplitude of tree-related HIF, the results of series of electrical conductivity measurements are employed to finite element model of tree and the maximum amplitude of tree-related high impedance fault is calculated. Then the obtained values from simulation were compared with those obtained from experiments in a real medium voltage network and the comparison results are shown in Table 2. As shown in Table 2, there is a relatively small absolute difference between measured and FEM values.

3.2 Maximum amplitude determination of high frequency component

Empirical mode decomposition technique is used to decompose original tree-related HIF to fundamental component and high frequency components. By applying the empirical mode decomposition method [17, 18], original tree-related HIF signals were decomposed to n IMFs and one residual. By merging IMFs of first to (n-1)th into one signal, the high frequency components were obtained. And fundamental component was achieved by merging nth IMF and residual part. The decomposition results for tree species are shown in Fig. 12.

Table 3 shows comparison between the levels of fundamental component to its high frequency components of tree-related HIF signal for three understudied species.

Using FEM analysis and according to the ratio of high frequency components' pulses to fundamental component, the estimated maximum amplitude for high frequency components of tree-related HIFs was calculated and given in Table 4.

Table 4. The estimated maximum amplitude for high frequency components

Species	The level of high frequency components (A)	
	FEM results	Experimental results
Walnut	0.0476	0.0424
Poplar	0.0276	0.0245

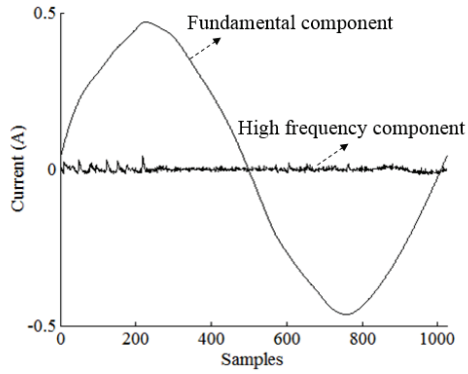

(a) Walnut tree

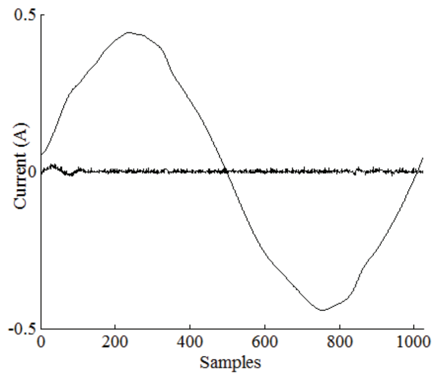

(b) Poplar tree

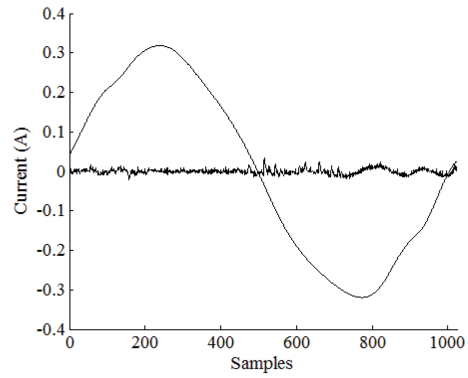

(c) Ash tree

Fig. 12. Fundamental component and high frequency components of tested trees

4. Tree-related High Impedance Fault Detection

High-frequency information contained within signal is what can distinguish tree-related HIFs from other similar events. So, in order to characterize tree-related HIFs, their high-frequency information should be evaluated to find a feature. For this purpose, high-frequency information contained within measured HIF signals were extracted employing empirical mode decomposition. Fig. 13 show the first and second IMFs for poplar, walnut, and ash tree. As evident in these figures, none of the functions have the same distribution. Pulse peak values are not also the same and there is no apparent relationship between IMFs. In other words, data related to IMFs are not actually distributed according to a given distribution, and had a lot of outliers that were far removed from the mean. Therefore, finding a common feature between them was not possible at this stage and other tools had to be employed. That is why quantile regression method [24] was chosen to find a unique feature for tree-related HIF. Indeed, the quantile regression method was employed to predict expected behavior of a tree-related HIF. This method is a powerful tool for real-time detection of abnormality in that it could capture the extreme values in data distribution of each IMF.

Q-quantiles are values that divide the group of discrete energy coefficients into q subsets of same sizes so that there are q−1 of the q-quantiles. The q-quantiles are the results of applying the inverse function of the cumulative distribution function to the values of $\left\{\frac{1}{q},\frac{2}{q},L,\frac{q-1}{q}\right\}$.

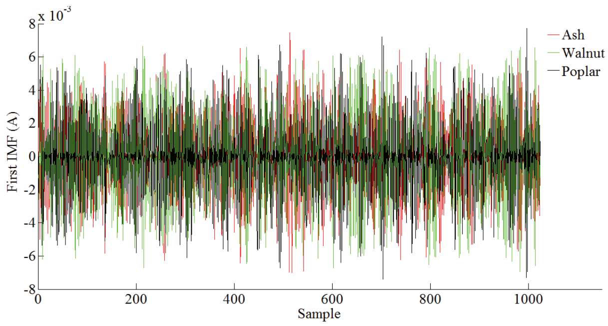

(a) First IMF

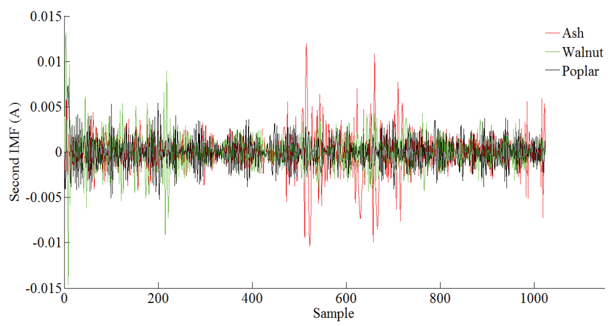

(b) Second IMF

Fig. 13. Distribution of intrinsic mode functions

In order to extract the feature contained within THIF currents, the relation between high frequency components and fundamental part of these signals have been evaluated in this paper. To find the relation between high frequency components and fundamental part of THIFs, specific trend between quantiles of them for different samples. According to the results of conducted evaluations, the following algorithm for tree-related HIF detection was extracted:

1. Measured THIF signal is decomposed according to the empirical mode decomposition algorithm [17, 18].
2. Intrinsic mode functions of first to nth are extracted.
3. The high frequency components coefficients of THIF are calculated by merging IMFs of first to (n-1)th and considered as a population.
4. Quantiles of each population are calculated according to the flowchart of Fig. 14.
5. The set of intervals for calculated quantiles is chosen.
6. The quantiles of the high frequency components distribution are plotted against the same quantiles of fundamental part distribution.
7. Linear regression between the quantiles is estimated.
8. The slope of estimated lines is calculated.
9. If the following conditions are met, the captured signal belongs to THIF:

- The quantiles-quantiles plot is symmetric, with deviations from straight line occurring in both the left and right tails
- The slope of the linear regression between the quantiles is s 0.01 with error margin of 0.009.
- Most of the points follow a linear pattern.
- There are a few outliers located at the extremes of the distribution and no outlier in the center of it.

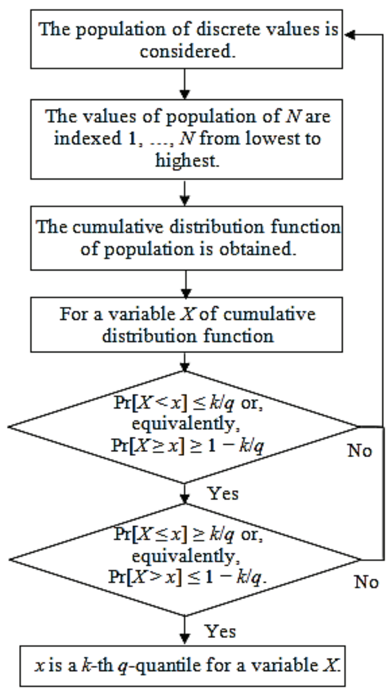

Fig. 14. Algorithm of Quantiles calculation

- The outliers depart upward from the straight line as you follow the quantiles to right side.
- The outliers depart downward from the straight line as you follow the quantiles to left side.

The results of applying proposed algorithm to different THIF signals are summarized as a series of scatterplots created by plotting two sets of quantiles related to high frequency components and fundamental part against one another (Fig. 15). These quantiles are the points in data below which a certain proportion of data fall and therefore can be utilized as an efficient index in detection targets. Superimposed on the plots are the lines joining the first and third quartiles of each distribution. These are the robust linear fits of the order statistics of the two distribution of

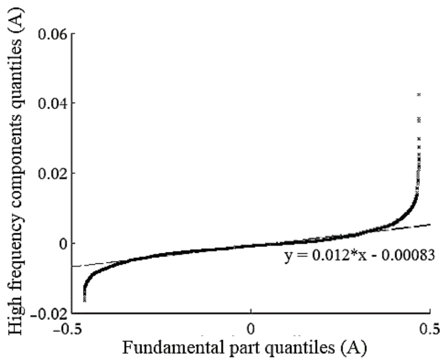

(a) Walnut tree

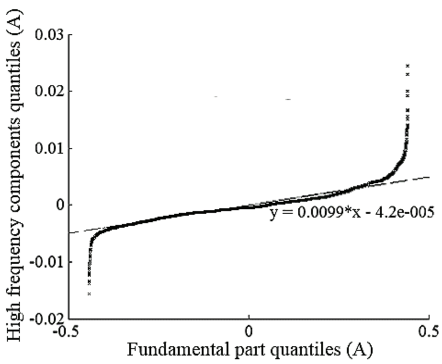

(b) Poplar tree

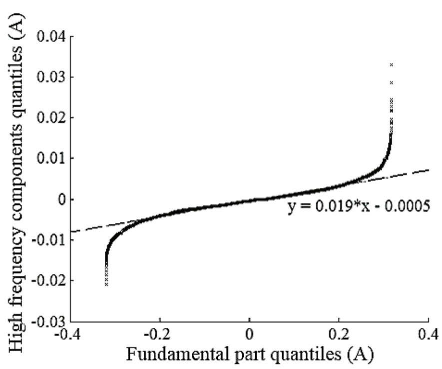

(c) Ash tree

Fig. 15. The quantile-quantile plots and estimated lines

high frequency components and fundamental part. These lines are extrapolated out to the ends of the sets and represent the specific trend between high frequency components and fundamental part. So, the slope of these lines indicates a specific feature of THIF.

As evident in scatterplots of Fig. 15, most of the data follow a linear pattern and is distributed on the center with two tails of data extending out to the left and right sides. However, a few outliers being evident at the extremes of the range reveal that some data of high frequency components and fundamental part are not distributed in the same manner. Some points depart upward from the straight line as you follow the quantiles to right and some depart downward as you follow the quantiles to left. The straight line illustrates where the points would fall if the high frequency components dataset were perfectly distributed the same as fundamental part dataset. The point's trend upward demonstrates that a few number of high frequency components quantiles are much greater than the fundamental part quantiles. And a contrasting phenomenon can be seen in left side in which the point's trend downward demonstrates that a few number of high frequency components quantiles are much lower than the fundamental part quantiles.

As shown in Fig. 15 and given that all the conditions stated in the algorithm have been met for all samples, THIF was accurately detected.

5. Conclusion

Vegetation coming into contact with overhead bare power lines can result in THIF that in turn can lead to property damage, electrical shock, power lines outage and in worst case widespread blackout. The main effective factor in such fault is electrical conductivity of vegetation's sap content which plays the role of an electrical conductor between the contact point and the ground. Therefore, in current paper, the electrical conductivity of vegetation's sap content was considered as a key indicator of THIF hazard.

Traditional methods used for vegetation monitoring in power lines corridors include time consuming and expensive field surveys which are not applicable in wide-area scale. Remote sensing techniques represent a fast cost-effective alternative approach to this kind of monitoring. Thus this paper proposed a method for estimating vegetation's electrical conductivity using spectral data derived from satellite imagery to help THIF risk assessments. For this purpose, the correlation between spectral data and field measurements of electrical conductivity of trees was modeled using regression analysis. Based on the obtained correlation function and FEM, the THIF current was estimated.

The findings of this paper could be applied as a mean for wide-area mapping of vegetation's electrical conductivity in power lines corridors at regular intervals with acceptable

Fig. 16. HIF experiment under 20 kV power lines

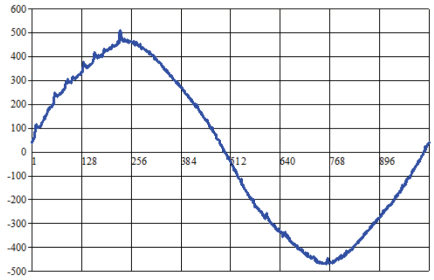

(a) Walnut Tree

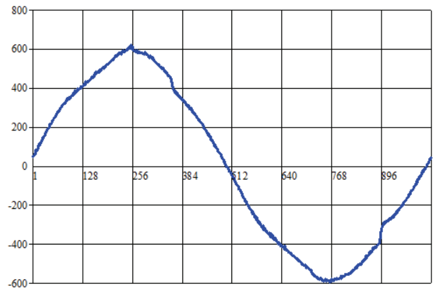

(b) Poplar Tree

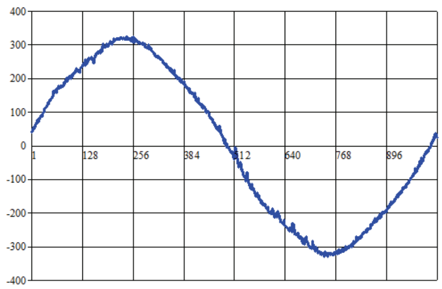

(c) Ash Tree

Fig. 17. Downloaded stored THIF current (mA)

accuracy. This cost-effective method provides a way to map THIF danger in power networks.

In summary, the original contributions of current research include 1) Using empirical mode decomposition in pre-processing of THIFs signals and extracting their main components, 2) Recommending quantile regression for the feature definition of THIF, 3) wide-area monitoring the electrical conductivity of live trees in the power lines' corridors using remote sensing, 4) Recommending a mathematical model for correlation between electrical conductivity of live trees and spectral indices, 5) Presenting an indicator of THIF hazard. 6) Considering the proposed THIF hazard indicator as a weight-coefficient in sensors' placement problem.

Appendix - Experimental Results of THIF

Several HIF experiments were performed on different species of trees under 20 kV power lines in Hamedan/Iran (Fig. 16). These species included Ash, Poplar and Walnut. The fault's current waveform of each species was captured by using a power analyzer that provides a high sampling rate of 1024 samples/period. Stored data were down loaded by laptop. The obtained results from THIF tests of different species on MV power lines are documented in Fig. 17.

References

[1] M. Adamiak, C. Wester, M. Thakur, C. Jensen, "High impedance fault detectionon distribution feeders," *GE Industrial Solution,* pp. 25-31, 2006.

[2] A. Milioudis, G. Andreou, and D. Labridis, "Enhanced protection scheme for smart grids using power line communications techniques — Part I: Detection of high impedance fault occurrence," *IEEE Trans. Smart Grid*, vol. 3, no. 4, pp. 1621-1630, 2012.

[3] Apostolos N. Milioudis, Georgios T. Andreou, Dimitris P. Labridis, "Detection and Location of High Impedance Faults in Multiconductor Overhead Distribution Lines Using Power Line Communication Devices," *IEEE Trans. Smart Grid*, vol. 6, pp. 894-902, 2015.

[4] T. Marxsen. "Power line bushfire safety program," Department of Economic Development, Jobs, *Transport and Resources*, Jul, 2015.

[5] J. R. Macedo, J. W. Resende, C. A. Bissochi, D. Carvalho, F.C. Castro, "Proposition of an inter harmonic-based methodology for high-impedance fault detection in distribution systems," *IET Gener. Transm. Distrib*. vol. 9, no. 16, pp. 2593-2601, 2015.

[6] L.U. Iurinic, A.R. Herrera-orozco, R.G. Ferraz, A.S. Bretas, "Distribution Systems High-Impedance Fault Location: A Parameter Estimation Approach," *IEEE Trans. Power Deliv*., vol. 31, pp. 1806-1814, 2016.

[7] N. Elkalashy, M. Lehtonen, H. Darwish, M. Izzularab, A.-M. Taalab, "Modeling and experimental verify-cation of high impedance arcing fault in medium voltage networks," *IEEE Trans. Dielectr. Electr. Insul*. vol. 14, no. 2, pp. 375-383, 2007.

[8] C. H. Kim, H. Kim, Y. Ko, S. H. Byun, R. K. Aggarwal and A. T. Johns, "A Novel Fault-Detection

Technique of High-Impedance Arcing Faults in Transmission Lines Using the Wavelet Transform," *IEEE Trans. Power Deliv*., vol. 17, no. 4, pp. 921-929, 2002.

[9] R. Paththamperuma, I. Perera, K. Perera, C. Perera, N. De Silva, U. Javatunga, "High Impedance Arcing Fault Detection in Low Voltage Distribution Network," *Digital Library of University of Moratuwa*, pp. 1-6, 2013.

[10] V.T.H.F.R.S. Maximov, J.L. Guardado, "High impedance fault locationformulation: a least square estimator based approach," *Math. Problems Eng*., p. 1-10, 2014.

[11] M. G. Ahsaee, "Accurate NHIF locator utilizing two-end unsynchronized measurements," *IEEE Trans. Power Del*., vol. 28, no. 1, pp. 419-426, 2013.

[12] W. Costa dos Santos, B. Alencar de Souza, N. Silva Dantas Brito, F. Bezerra Costa, M. Renato Cerqueira PaesJr "High Impedance Faults: From Field Tests to Modeling", *in Journal of. Control, Automation and Electrical Systems*, vol. 24, no. 6, pp. 885-896, 2013.

[13] A. Mahari, H. Seyedi, "High impedance fault protection in transmission lines using a WPT-based algorithm," *Int. J. Electr. Power Energy Syst*. vol. 67, pp. 537-545, 2015.

[14] P. Biradar, V.R. Sheelvant, "High-impedance fault detection using wavelet transform," *Int. J. Eng. Res. Gen. Sci*., pp. 166-173, 2015.

[15] N.R. Varma, D.B.V.S. Ram, D.K.S.R. Anjaneyulu, "Development of fault detection algorithm for high impedance faults in distribution network using multiresolution analysis," *Int. J. Eng. Res. Technol*. vol. 3, no. 9, pp. 573-576, 2014.

[16] I. Baqui, I. Zamora, J. Mazón, G. Buigues, "High impedance fault detection methodology using wavelet transform and artificial neural networks," *Electr. Power Syst. Res*. vol. 81, no. 7, pp. 1325-1333, 2011.

[17] M. A. Azpúrua, M. Pous, F. Silva, "Decomposition of Electromagnetic Interferences in the Time-Domain," *IEEE Trans. Electromagn. Compat*., vol. 58, no. 2, pp. 385-392, 2016.

[18] J. C. Chan, H. Ma, T. K. Saha, "Self-adaptive partial discharge signal de-noising based on ensemble empirical mode decomposition and automatic morphological thresholding", *IEEE Trans. Dielectr. Electr. Insul*, vol. 21, pp. 294-303, 2014.

[19] A. Ghaderi, H.A. Mohammadpour, H. Ginn, High impedance fault detectionmethod efficiency: simulation vs. real-world data acquisition, in: Power and Energy Conference at Illinois (PECI), *2015 IEEE*, pp. 1-5, 2015.

[20] F. Namdari, N. Bahador, "Modeling trees internal tissue for estimating electrical leakage current," *IEEE Trans. Dielectr. Electr. Insul*., vol. 23, pp. 1663-1674, 2016.

[21] F. Namdari, N. Bahador, "Modeling trees internal tissue for estimating electrical leakage current," *In Progress: IET Gener. Transm. Distrib*., Aug. 2017.

[22] R.K. Sairam, K.R. Veerabhadra, G.C. Srivastava. "Differential response of wheat genotypes to long-term salinity stress in relation to oxidative stress, antioxidant activity and osmolyte concentration," *Plant Sci*., vol. 163, pp. 1037-1046, 2002.

[23] G.G. Aseyev. "Supramolecular Interactions and Non-Equilibrium Phenomena in concentrated solutions Georgii Georgievich Aseyev," *CRC Press*, 2014.

[24] N. R. Bahador, F. Namdari. And H. R. Matinfar, "Feature extraction of tree-related high impedance faults as a source of electromagnetic interference around medium voltage power lines' corridors," Progress In Electromagnetics Research B, vol. 75, pp. 13-26, 2017.

Nooshin Bahador was born in Hamedan, Iran on 1988. She received the B.Sc. degree in electrical engineering from Buali Sina University, Iran in 2010. She was awarded the M.Sc. degree from Shahrood University of technology in 2013. Currently, she is working towards the Ph.D. degree at Power Ing, Lorestan University.

Hamid Reza Matinfar was born in Hamedan, Iran, 1969. He received his B.Sc. in 1992 in soil sci. of university of Tehran, M.Sc. in 1995 in soil sci. of university of Tehran, Iran, and Ph.D. in 2006 at university of Tehran in soil sci.

Farhad Namdari was born in Khoramabad, Iran, 1972. He received his B.Sc. in 1995 at the Iran University of Science and Technology (IUST), M.Sc. in 1998 at the Tarbiat Modarres University (TMU), Iran, and Ph.D. in 2006 at the IUST all in Electrical Power Engineering. He is an Assistant Professor with the Department of Electrical Engineering at Lorestan power system protection, smart grids, power system operation and control, and Artificial Intelligent (AI) techniques in power systems.